JOURNAL OF THERMOPHYSICS AND HEAT TRANSFER
Vol. 9, No. 1, January–March 1995

# Spray Cooling of Power Electronics at Cryogenic Temperatures

Maninder S. Sehmbey,* Louis C. Chow,† Ottfried J. Hahn,‡ and Martin R. Pais§
*University of Kentucky, Lexington, Kentucky 40506*

**The operation of power electronics at liquid nitrogen temperature (LNT) is a very attractive possibility. However, a high heat flux (over 1.0 × $10^6$ W/m$^2$) cooling technique, like spray cooling, will have to be used to realize all the advantages of low-temperature operation. This study details the results from experiments conducted to study the heat transfer characteristics during spray cooling with liquid nitrogen. Four different nozzles at various pressures were used to study the variation in spray cooling heat transfer at LNT. The effect of nozzle and flow rate on the critical heat flux and overall heat transfer characteristics are presented. Heat fluxes close to 1.7 × $10^6$ W/m$^2$ were realized at temperatures below 100 K. The mass flow rate range was from 6.1 × $10^4$ kg/h·m$^2$ to 3.2 × $10^5$ kg/h·m$^2$.**

## Nomenclature

$q''$ = heat flux, W/m$^2$
$T_{sat}$ = saturation temperature, K
$T_w$ = surface temperature, K

## Introduction

THE operation of electronics at liquid nitrogen temperature (LNT) has become very attractive due to the development of high-temperature superconductors (HTSs) and the fact that many metal-oxide semiconductor (MOS) devices operate better at LNT.

Superconducting circuits will consist of HTS devices (logic gates, inverters, memory cells, etc.) with superconducting interconnects.[1] Almost all of the functions performed in high-performance electronics can be done by a superconductor circuit.[2] However, superconductor circuits cannot handle high power levels; also, there are no superconducting rectifiers, and semiconductors make better amplifiers and mass memory devices.

A cursory examination of heat transfer requirements in superconducting circuits may lead one to believe that due to the very nature of superconductivity heat dissipation would not be a problem. A closer examination, however, reveals how ill-founded that notion is. The main components in a superconducting circuit are the high-speed, low-power switches, the Josephson junctions [also called superconductor-insulator-superconductor devices (SISs)].[3-7] The main advantages of these devices are the low gate delay times and low power dissipation; these features in combination will allow much higher device packing compared to semiconductor circuits. However, the thermal management aspect of superconducting circuits at LNT has been of concern lately.[8,9] A typical SIS working at 4.2 K has a power dissipation of 5 × $10^4$ W/m$^2$, however, for operation at 77 K, the same device may have a heat dissipation approaching 6.0 × $10^6$ W/m$^2$.[9,10] Obviously, this level of heat dissipation cannot be handled by common heat removal techniques. Hence, superconducting circuits at LNT would require lower device density and a high heat removal technique for thermal management.

Many investigators have reported that MOS semiconductor devices show a marked improvement in performance as the operating temperature is lowered.[1,2,8,11,12] Furthermore, the thermal conductivities of semiconductor substrates and packaging materials (silicon, germanium, beryllium, alumina) are seen to increase dramatically as the temperature is lowered to LNT.[13] The main advantages of low-temperature operation are, increased electron and hole mobilities, lowered interconnection resistivities, reduced leakage currents, greater subthreshold slope, and reduction in thermal noise.[11] One of the possible applications of low-temperature electronics will be in the area of high efficiency ac/dc, dc/ac, and rf power conversion at the multikilowatt level. As mentioned earlier, superconducting circuits are not capable of handling high power levels. Hence, MOS field effect transistors (MOSFETs) can be used in combination with high $Q$ inductors and capacitors made from HTSs to obtain the zero voltage switching circuits suitable for power conversion applications. Such an integration will result in a drastic size and weight reduction. The efficiency of these circuits improves greatly at low temperatures due to the dramatic reduction in the on-resistance of power MOSFETs.[12] However, the efficiency of these circuits depends greatly on the $Q$ values of the inductors and capacitors used in the circuit. Hence, it is necessary to use HTSs for these components to obtain the maximum efficiency. However, even at this increased efficiency, the heat dissipation from the multikilowatt circuits will require a high heat flux removal technique.[12] Other types of hybrid circuits, taking advantage of the best features of semiconductors and superconductors, are also under development.[1,2,8] Any hybrid circuit is inherently more prone to thermal failure due to the presence of high heat dissipation transistors in the vicinity of superconducting elements. Hence, it is essential that the cooling system be capable of removing high heat fluxes to prevent any hot spots and the resultant device failure.

All this has led to the interest being focused on spray cooling as the high heat flux removal technique. Spray cooling as a way of efficiently removing heat from a surface has been around for some time now. Liquid nitrogen (LN2) spray has been used in food storage industry to rapidly and efficiently freeze perishable goods. Spray cooling with water has found use in cooling steel forgings. All of these uses, however, have involved surfaces with much higher temperatures as compared to the fluid used for spray cooling. At these temperatures the fluid does not wet the surface, and the heat transfer is by the process of conduction through the thin film of vapor that exists between an impinging droplet and the hot surface. Spray cooling has proven very effective in this type of cooling because the momentum of the droplets allows the liquid to get much closer to the surface than it would if the surface were just

Received Nov. 24, 1993; revision received May 1, 1994; accepted for publication May 11, 1994. 

*Associate Engineer, Department of Mechanical Engineering. Member AIAA.
†Professor, Department of Mechanical Engineering. Associate Fellow AIAA.
‡Professor, Department of Mechanical Engineering.
§Associate Research Professor, Department of Mechanical Engineering. Member AIAA.

immersed in the liquid. The phenomena involved in this form of spray cooling have been widely studied.[13-15] This form of spray cooling has a low heat transfer coefficient $h$, and thus, is not very useful for applications that involve high heat fluxes. However, when the same spray impinges upon a surface with a temperature slightly higher than the liquid temperature, we find that very high heat transfer coefficients are attained.[16-18] If we compare spray cooling to the other cooling methods we find that the heat transfer coefficients are significantly higher. For instance, pool boiling with water has $h \sim 5 \times 10^4$ W/m$^2$·K, whereas for spray cooling using water, $h$ over $5 \times 10^5$ W/m$^2$·K has been observed.[18] Another major advantage of spray cooling is that much higher heat fluxes can be achieved at relatively low surface temperatures (i.e., high critical heat flux). Spray cooling with water has been shown to be capable of removing close to $1.0 \times 10^7$ W/m$^2$ at temperatures lower than 140°C under normal surface conditions.[16-18] For very smooth surfaces heat fluxes higher than $1.0 \times 10^7$ W/m$^2$ have been achieved at a surface temperature lower than 105°C, using water as the coolant.[17] These numbers can be better appreciated when compared to the highest heat flux achievable in the saturated pool boiling of water: ~$1.0 \times 10^6$ W/m$^2$ at 120°C.

Most of the earlier spray cooling research involved low heat fluxes and low fluid flow rates.[19,20] In the past few years a significant amount of work has been done in high heat flux spray cooling research.[16-18,21-23] The complexity of the phenomena involved have, however, frustrated attempts to successfully model the process. Also, the effect of various spray parameters on the heat transfer characteristics is difficult to differentiate because most spray parameters are related to each other. For example, for a particular nozzle, an increase in nozzle pressure causes an increase in spray velocity and mass flow rate, and, a decrease in the mean droplet diameter.[24] Because the spray cooling heat transfer process is not well understood, the correlations offered by previous researchers are applicable only under the specific conditions of that study. A comprehensive predictive correlation/model for spray cooling is still not available.

Hence, the main objective of this study is to obtain the heat transfer characteristics of spray cooling with liquid nitrogen. This is done by experimentally obtaining heat transfer data for LN2 spray cooling under different spray conditions. The following sections describe the experimental setup, procedure, and results.

## Experiment Setup

The schematic diagram of the setup is shown in Fig. 1. The experimental chamber contains the heater, nozzle, and view ports. The high-pressure LN2 dewar is used to supply liquid nitrogen to the nozzle. A heat exchanger between the dewar and the nozzle is used to subcool the high-pressure liquid down to about 78 K. Since the chamber is always maintained at atmospheric pressure, the liquid spraying out of the nozzle is always close to saturation if the upstream temperature is maintained at about 78 K (assuming isentropic expansion). All the lines were insulated with polyurethane foam to minimize heat gain. During preliminary experiments, it was found that, at low flow rates, it was very difficult to maintain a single-phase fluid supply into the nozzle inlet, this resulted in violent pressure fluctuations and eventual disruption of flow. This happened because the heat gain into the line was sufficient to vaporize a part of the liquid flow at low flow rates. In order to overcome this problem, a bleed port was provided just prior to the nozzle. Thus, the total flow through the line could be maintained high enough to prevent vaporization. The bleed flow was vaporized by passing it through a long heat exchanger tube coil placed in a hot water bath. The bleed flow was continuously monitored by a mass flow meter measuring the flow rate of gaseous nitrogen exiting the heat exchanger.

The heater, shown in Fig. 2, is made out of oxygen-free copper; a cartridge heater inserted inside the copper block provides the heat. The power to the cartridge heater is supplied by a variac. The heat transfer surface is a 1-cm$^2$ circle on the top of the block. A cylindrical Teflon® gasket was fitted onto the top part of the block. The fit between the Teflon gasket and the copper block was very tight and provided a very good seal against liquid leakage into the interface. The top surface of the block (the heat transfer surface) was made flush to the top surface of the Teflon gasket as shown in the figure. Two thermocouples in the copper block below the heat transfer surface measure the temperature gradient below the surface. The optimum thermocouple distance from the surface was obtained by thermal design using finite element analysis software by Swanson Analysis Systems, Inc. (ANSYS). The thermocouple distance was sufficient to enable extrapolation of the average surface temperature, even if a moderate lateral temperature gradient existed on the surface (a 5 K lateral gradient was used to obtain the design values). The heat flux and the average surface temperature are estimated from these thermocouple measurements. All surfaces of the heater block, except the top, are insulated using polyurethane foam (thermal conductivity: 0.035 W/m·K) to prevent heat loss. The heat loss from the block was estimated to be less than 2% with this insulation (based on calculations assuming that the outer surface of the insulation is at LN2 temperature). The heat input from the cartridge heater is determined by measuring the power input to the heater using a power transducer. This measurement was used to confirm the heat flux calculated from the temperature gradient and validate those calculations.

In addition to those in the copper block, thermocouples were also placed on the insulation surface, inside the chamber, on the nozzle body, in-stream near nozzle inlet, in the subcooling heat exchanger, and on the chamber surface. The liquid flow rate to the nozzle is calculated by subtracting the bleed flow rate from the flow rate measured by the orifice-

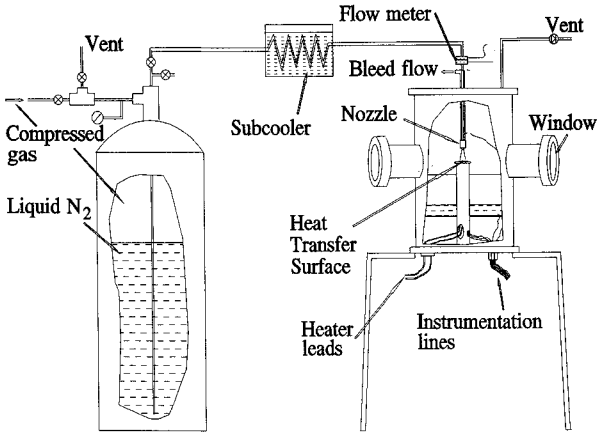


Fig. 1 Experimental setup.

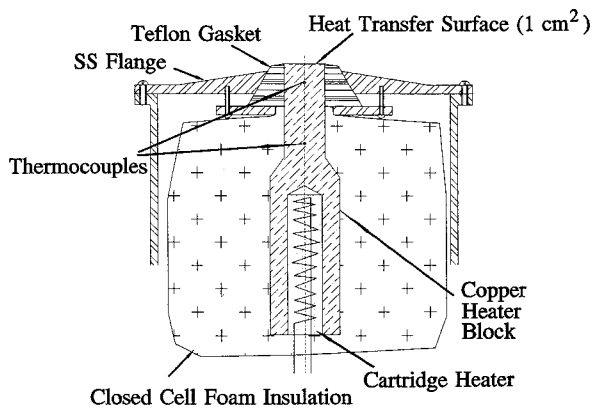


Fig. 2 Heater details.

flow meter shown in Fig. 1. All of the thermocouples and the power transducer output were read by a Fluke Helios Plus data acquisition system connected to a PC. During the experimental runs, all data was recorded by the computer.

## Experimental Procedure

An experimental run involved spraying the LN2 at a certain pressure and 78 K through the nozzle onto the heater surface. The roughness of the heater surface was measured before the heater was installed in the chamber, and also at the conclusion of the whole set of experiments. The roughness was measured by a surface profilometer (Surtronics 3P, Rank Taylor-Hobson, Ltd.), and was around $R_a = 0.15$ $\mu$m, both before and after the experiments. The surface was cleaned with a very dilute solution of hydrochloric acid and then rinsed with deionized distilled water and propanol prior to each set of experiments. Before beginning the experiment, the chamber is flushed with nitrogen to expel any air or water vapor. The subcooling heat exchanger shell is filled with LN2 and the fluid is allowed to flow from the dewar to the nozzle. The bleed port is kept fully open till the line cools down to LN2 temperature. This is evidenced by the temperature of the nozzle reaching 78 K. The pressure of the dewar is then set at the desired value by venting the dewar or pressurizing it from a N2 gas cylinder. The bleed valve is adjusted until the bleed flow is as low as possible but is still sufficient to maintain the nozzle temperature at 78 K. The bleed flow rate never exceeded $4.0 \times 10^4$ kg/h·m$^2$. The nozzle height and alignment is adjusted to ensure that the spray covers the whole heat transfer surface, and all the spray impinges the surface.

The power to the heater cartridge is then increased gradually until dryout of the surface occurs. After each step increase in power, sufficient time is allowed for all the temperatures to reach steady state. The power to the heater is cut off immediately following the dryout. Dryout is evidenced by the rapid increase in temperature readings of the two thermocouples inside the copper block. Upon dryout, the temperature of the surface usually reaches about 200 K because of the thermal inertia of the heater block. The data recording is continued until the surface temperature falls back to about 80 K under the same spray conditions. Although these cooldown readings are not at steady state, the correct heat flux and surface temperature can be estimated by correcting for the temperature transients. The cooldown readings provide the heat transfer characteristics for LN2 spray cooling in the Leidenfrost point region.

In general, a set of runs were taken consecutively until the LN2 in the dewar ran out, or, the nozzle had to be changed. The set of results presented here involved four nozzles: 1) TG0.3, 2) TG0.5, 3) TG0.7, and 4) FL#13. The TG series nozzles are full cone pressure atomizing nozzles commercially available from Spraying Systems Co., Wheaton, Illinois. These nozzles have a flow swirler before the orifice that creates turbulent flow for effective atomization. The FL#13 is a flat disc-shaped nozzle with radial grooves leading to the orifice (for creating turbulence). The orifice diameters for these nozzles are presented in Table 1.

The experiments were carried out for five to six different pressures for each nozzle (207, 276, 414, 552, 690, and 828 kPa). The nozzle inlet pressure was continuously monitored by a Bourdon gauge connected to the low-pressure side of the orifice-meter. The spray cone for the FL#13 nozzle (about 40 deg) was much narrower than that for the TG series nozzles (about 60 deg). The nozzle height above the surface was varied to keep the surface covered with spray, all the experiments with TG series nozzles had approximately the same nozzle height: 1 cm; the height for the FL#13 nozzle was about 1.6 cm. The nozzle height was adjusted such that the spray cone hit the whole surface and did not extend beyond it. All the nozzles used in this study had no nonuniformities in the angular direction (i.e., the spray cones always had a circular cross section).

**Table 1 Nozzle size**

| Nozzle | Orifice diameter, mm |
|---|---|
| TG0.7 | 0.76 |
| TG0.5 | 0.61 |
| TG0.3 | 0.51 |
| FL#13 | 0.38 |

## Results and Discussion

A brief discussion of spray cooling theory will provide a better insight into the results presented here. Figure 3 shows the probable mechanisms involved in spray cooling heat transfer. Convection heat transfer, evaporation from the film surface, nucleate boiling at the heater surface, and secondary nucleation are all thought to be involved in spray cooling. The intense convection caused by impinging droplets enhances the heat transfer between the heater surface and the free surface of liquid film, the heat transferred to the film surface goes towards evaporation of the fluid. Nucleate boiling at the heater surface with premature bubble removal also helps in increasing the heat transfer coefficient greatly. Since a spray with high-speed droplets is subjected on the liquid film surface, the bubbles growing in the liquid film are unlikely to survive once their size approaches the liquid film thickness. Thus, the bubbles can break up at a very small size, even before the microlayer[25,26] is completely evaporated. This bypasses the much longer and less efficient growth period in pool boiling where the bubble has to grow slowly after microlayer evaporation in order to attain enough volume for the buoyancy forces to overcome the surface tension forces holding the bubble to the surface. The overall effect of this premature bubble breakup is to increase the net time the microlayer evaporation exists on a surface, and thereby increase the heat transfer coefficient. Finally, secondary nucleation, which results from the entrapment of vapor bubbles by impinging liquid droplets, also play a very important role in spray cooling.[27,28] The term secondary nucleation was coined to describe the nuclei from the vapor entrained by the re-entering droplets created by bubbles bursting out of the liquid film. Due to the lack of a better term, and due to the fact that the phenomenon is similar whether the droplets originate from the liquid film or from an external source (spray in this case), we refer to nucleation due to vapor entrained by the spray as secondary nucleation. Also, due to the very high number density of spray droplets impinging on the liquid film, the dominant source of this secondary nucleation is the spray itself. The heat transfer due to secondary nucleation would be less efficient as compared to microlayer evaporation since the thickness of liquid between a secondary nucleus and the heat transfer surface is larger than the microlayer thickness. Although it is conceivable that a bubble due to a secondary

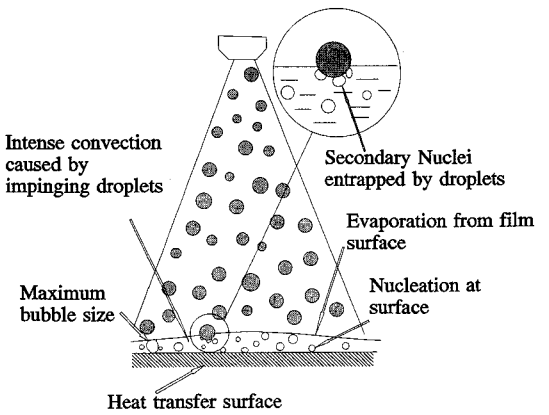


**Fig. 3 Spray cooling.**

nucleus can get close enough to the heat transfer surface to permit microlayer evaporation, the time for this type of microlayer evaporation is unlikely to approach that experienced by a bubble originating from a surface cavity. Hence, it is safe to assume that bubbles originating from surface cavities remove heat more efficiently as compared to bubbles originating away from the surface.

The relative importance of each of these heat transfer mechanisms is unknown to date, but in spite of the lack of that information, the hypothesis provides a useful tool for evaluating the experimental results. Also, the experimental data will help in resolving the various issues involved in the hypothesis. Another point that has to be stated is that the hysteresis phenomenon, which is quite common in boiling from surfaces in highly wetting liquids like chlorofluorocarbons and cryogens, is not expected to occur in spray cooling. This is due to the fact that the presence of secondary nucleation facilitates phase change at very low superheat, and thus prevents the temperature overshoot that occurs due to deactivation of nucleation sites on the surface.

The results for each nozzle are presented first, and then comparisons are made based on the mass flow rate and nozzle type. All the TG series nozzles have some degree of nonuniformity in spray, the spray cone is usually less dense along the axis compared to the edge. This nonuniformity is not very severe and the center of spray has sufficient droplets to prevent liquid dearth in the center.

The TG0.3 had the smallest orifice of all the TG series nozzles used in this study. The spray for this nozzle was dense overall and slightly less dense along the axis. Figure 4 shows the superheat ($T_w - T_{sat}$) vs heat flux data for three different flow rates (or nozzle pressures). As seen from the figure, the heat transfer curve is made up of three distinct regions. The first is the low superheat region, here, the heat transfer is probably dominated by forced convection with evaporation from the film surface, and secondary nucleation.

Nucleate boiling from the surface is absent in the first region because surface nucleation requires a higher superheat in forced convection situations.[29] On the other hand, boiling due to secondary nucleation can exist from a very low superheat and would be undeterminable from the heat transfer curve in this case. As the superheat is increased, it is seen that the slopes of the curves show a small jump at about 9 K superheat, this is probably due to the beginning of nucleate boiling from cavities on the heater surface. As mentioned earlier, nucleation from the surface cavities allows microlayer evaporation and, hence, higher heat transfer coefficient as compared to a nuclei originating in the liquid film. Therefore, this shift in slope could be attributed to the boiling from nucleation sites on the surface.

Once the nucleate boiling from the heater surface has begun, the curves in Fig. 4 show a definite shift upwards, this second region can be said to have a significant contribution by surface nucleation. Upon reaching a superheat of about 15 K, the curves in Fig. 4 become almost horizontal, this is due to the partial dryout of the surface. As mentioned earlier, the spray is less dense along the axis, hence, the dryout starts on the center of the surface (due to lower mass flux at the center) and progresses outward. This shows up as a gradual increase in average surface temperature with almost no increase in heat flux. When the surface is fully dry, the surface temperature jumps to a higher value and the heat input is shut off. The block then begins to cool down under Leidenfrost conditions, the heat flux under these conditions is around $1.5–3.0 \times 10^5$ W/m$^2$ for the cases shown in Fig. 4. A complete curve for the full temperature range is shown in Fig. 5. As seen from the figure, the heat flux reaches a minimum at a superheat of around 45 K and then starts rising rapidly as the droplets begin to wet the surface.

The influence of mass flow rate on heat transfer characteristics is quite clear from Fig. 4; the critical heat flux (CHF) and heat transfer coefficient increase with an increase in mass

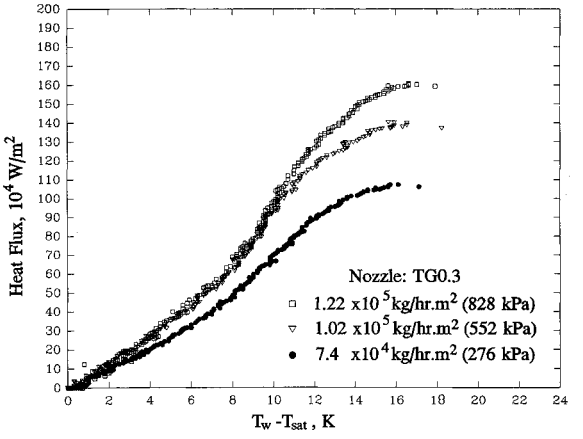


**Fig. 4 TG0.3 heat transfer characteristics.**

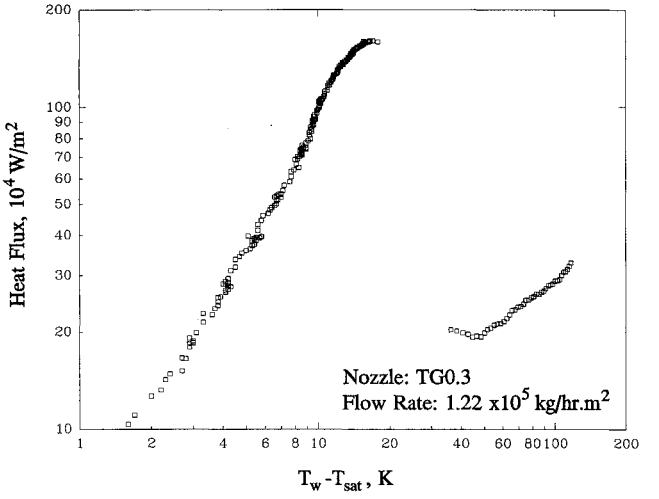


**Fig. 5 Typical characteristics for full temperature range.**

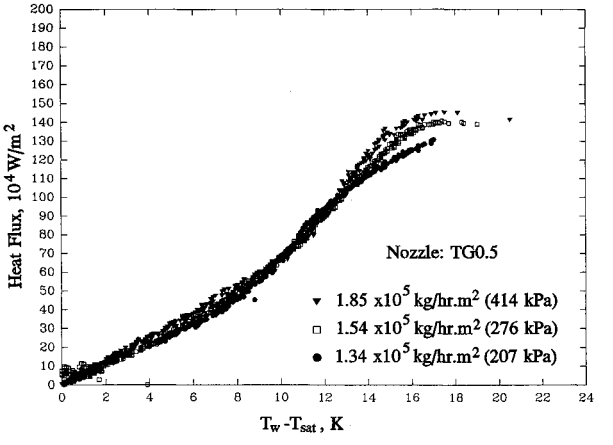


**Fig. 6 TG0.5 heat transfer characteristics.**

flow rate. This effect is more pronounced for CHF, where a more significant increase is seen with increase in flow rate.

Figure 6 shows the heat transfer characteristics for spray cooling with the TG0.5 nozzle. The trends are similar to those described for the TG0.3 nozzle. The increase of mass flow rate leads to an increase in CHF. However, the change in mass flow rate does not seem to have a significant effect on the heat-transfer coefficient. The spray from this nozzle was also less dense along the axis, hence, a short third region exists in this case too.

The spray from the TG0.7 nozzle was also very dense overall, and slightly less dense in the middle. Figure 7 shows the heat transfer characteristics for this nozzle. The trends in the

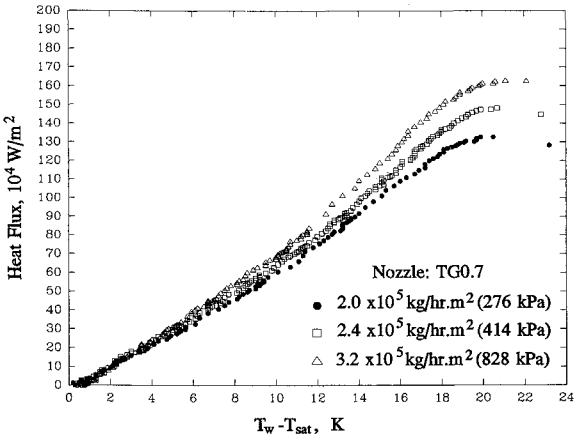


Fig. 7 TG0.7 heat transfer characteristics.

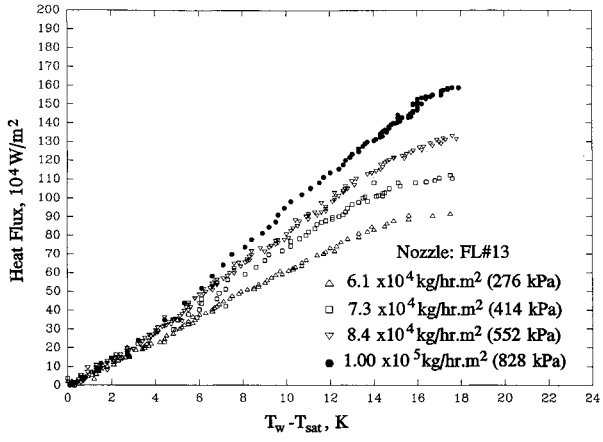


Fig. 8 FL#13 heat transfer characteristics.

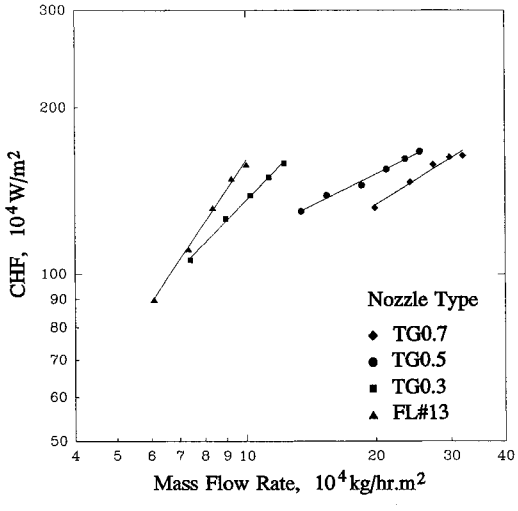


Fig. 9 Effect of nozzle and mass flow rate on CHF.

curves and mass flow rate effect are similar to the previous case. However, very little change in the slope of the curve is observed. Thus, there appears to be very little surface nucleation in this case. This could be due to some minor variation in surface conditions. As mentioned earlier, the surface roughness was the same throughout these experiments, however, the presence of oxide layer on the surface in some cases cannot be ruled out. Although the surface was cleaned before each set of experiments, it is difficult to visually detect a very thin oxide layer that could have been left on the surface. However, this explanation is extended only due to the lack of any other apparent reason for this behavior.

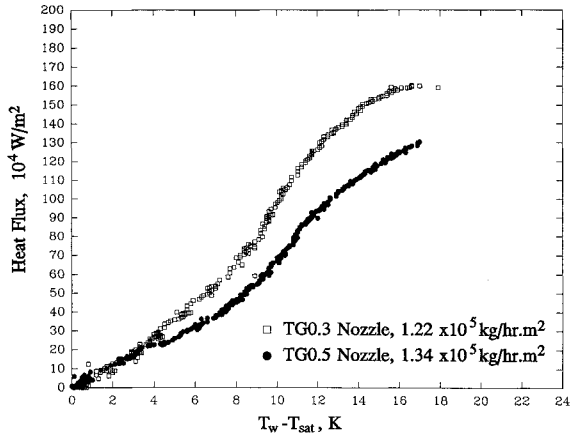


Fig. 10 Effect of nozzle on heat transfer.

Figure 8 shows the heat transfer characteristics for the FL#13 nozzle. This nozzle had the smallest orifice diameter, and hence, the lowest flow rate at any particular pressure. The spray from this nozzle was very well distributed, and the nonuniformity was not noticeable from a visual observation. As can be seen from Fig. 8, the different flow rate curves for this nozzle are more distinguishable from each other compared to the other cases. This indicates that the influence of mass flow rate on heat-transfer coefficient is greater at very low flow rates. The increase in heat-transfer coefficient and CHF with increase in mass flow rate is clearly evident. Again, as was the case for the TG0.7 nozzle, very little shift in the heat transfer curve is observed.

Since the effect of flow rate on CHF is most pronounced for all cases, the CHF vs mass flow rate characteristics for different nozzles are compared first. This comparison is shown in Fig. 9. As is clearly evident from the figure, all nozzles show an increase in CHF with an increase in mass flow rate. However, the increase is nonlinear, i.e., there is a diminishing increase in CHF with increase in mass flow rate.

From looking at Fig. 9 it is apparent that the efficiency of spray cooling increases as the nozzle size is decreased. In fact, the highest CHF attained (for the pressure range examined here) for all four nozzles is almost the same; the highest CHF for the smallest nozzle (FL#13) was about $1.60 \times 10^6$ W/m$^2$ at a flow rate of $1.00 \times 10^5$ kg/h·m$^2$, whereas the highest CHF for the largest nozzle (TG0.7) was about $1.65 \times 10^6$ W/m$^2$ at a flow rate three times as high ($3.20 \times 10^5$ kg/h·m$^2$). The higher efficiency of smaller nozzles is probably due to the following reasons:

1) The flow rate obviously decreases with nozzle size, this leads to thinner liquid film[16] with decrease in nozzle size. The thinner liquid film results in lesser thermal resistance to heat transfer from the heater surface to the free surface of liquid film, this in turn leads to more evaporation from the film surface.

2) The velocity of the droplets increases with decrease in nozzle size,[24] this leads to higher convection heat transfer.

3) Most importantly, the number of droplets per unit area per unit time increases with decrease in nozzle size for same mass flow rate.[24] This would result in an increase in secondary nucleation and convection in the liquid film. These effects cannot be quantified until the spray characteristics are known.

The comparison of heat transfer characteristics for any two nozzles is more valid if the mass flow rates are the same, this eliminates the film thickness effect from consideration. Figure 10 shows a comparison of TG0.5 and TG0.3 nozzles at a similar flow rate. It can be seen that the heat transfer coefficient and CHF is higher for the TG0.3 nozzle, this clearly shows the effect of spray parameters on heat transfer characteristics and points to the need of measuring them. The effect of surface parameters also needs to be investigated before a comprehensive correlation can be formulated.

## Conclusions

Experiments were carried out to study the heat transfer characteristics of liquid nitrogen spray cooling with four nozzles at various flow rates. The critical heat flux was seen to increase with mass flow rate for any particular nozzle. The heat transfer coefficient generally increased with increase in mass flow rate for a particular nozzle. The highest heat flux obtained was around $1.65 \times 10^6$ W/m$^2$ at a superheat of approximately 16 K. Upon comparing the heat transfer characteristics for the different nozzles at similar flow rates, it was found that the CHF and heat transfer coefficient increases as the orifice size of the nozzle decreases. This is attributed to the increase in the number of droplets and the velocity of the droplets with decrease in orifice size. The spray parameters have to be measured in order to gain a better understanding into the process and formulate a correlation. This work is currently under progress and would be an extension of this study.

## Acknowledgments

This work was supported by the Wright-Patterson Air Force Base, Dayton, Ohio, Contract F33615-91-C-2152. Micheal Morgan was the technical monitor. The assistance of Austin Pyle and Sylvan Ferrell from the workshop is also appreciated.

## References

[1]Nisenhoff, M., "Superconducting Electronics: Current Status and Future Prospects," *Cryogenics*, Vol. 28, No. 1, 1988, pp. 47–56.

[2]Van Duzer, T., "Superconductor-Semiconductor Hybrid Devices, Circuits and Systems," *Cryogenics*, Vol. 28, No. 8, 1988, pp. 527–531.

[3]Van Duzer, T., "Josephson Digital Devices and Circuits," *IEEE Transactions on Microwave Theory and Techniques*, Vol. MTT-28, No. 5, 1980, pp. 490–500.

[4]Tucker, J. R., "Quantum Limited Detection in Tunnel Junction Mixers," *IEEE Journal of Quantum Electronics*, Vol. QE-15, 1979, pp. 1234–1258.

[5]McGrath, W. R., Raisanen, A. V., Richards, P. L., Harris, R. E., and Lloyd, F. L., "Accurate Noise Measurements of Superconducting Quasiparticle Array Mixers," *IEEE Transactions on Magnetics*, Vol. MAG-21, No. 2, 1985, pp. 212–221.

[6]Clarke, J., "Superconducting Quantum Interference Devices for Low Frequency Measurements, Superconducting Applications," *SQUIDs and Machines*, edited by B. R. Schwartz and S. Foner, Plenum Press, New York, 1977, pp. 67–124.

[7]Silver, A. H., and Zimmerman, J. E., "Quantum States and Transition in Weakly Connected Superconducting Rings," *Physics Review*, Vol. 157, 1967, pp. 317–341.

[8]Flik, M. I., and Hijikata, K., "Approximate Thermal Packaging Limit for Hybrid Superconductor-Semiconductor Electronic Circuits," *Proceedings of the 9th International Heat Transfer Conference* (Jerusalem, Israel), Vol. 2, Hemisphere, New York, 1990, pp. 319–324.

[9]Lavine, A. S., and Bai, C., "An Analysis of Heat Transfer in Josephson Junction Devices," *Journal of Heat Transfer*, Vol. 113, 1991, pp. 535–543.

[10]Van Duzer, T., "Superconductor Electronic Device Application," *IEEE Journal of Quantum Electronics*, Vol. QE-25, No. 11, 1989, pp. 2365–2377.

[11]Fox, R. M., and Jaeger, R. C., "MOSFET Behavior and Circuit Considerations for Analog Applications at 77 K," *IEEE Transactions on Electron Devices*, Special Issue on Low-Temperature Semiconductor Electronics, Vol. ED-34, No. 1, 1987, pp. 114–123.

[12]Mueller, O., "Cryogenic Power Conversion: Combining HT Superconductors and Semiconductors," *Superconductivity and Its Applications*, edited by Y. H. Kao, A. E. Kaloyeros, and H. S. Kwok, American Inst. of Physics, New York, 1991, pp. 746–759 (AIP 251).

[13]Deb, S., and Yao, S. C., "Heat Transfer Analysis of Impacting Dilute Spray on Surfaces Beyond the Leidenfrost Temperature," American Society of Mechanical Engineers National Heat Transfer Conf., Paper 87-HT-1, Pittsburgh, PA, 1987.

[14]Wachters, L. H. J., Bonne, H., and Van Nouhuis, H. J., "The Heat Transfer from a Hot Horizontal Plate to Sessile Water Drops in the Spheroidal State," *Chemical Engineering Science*, Vol. 21, 1966, pp. 923–936.

[15]Awonorin, S. O., "Film Boiling Characteristics of Liquid Nitrogen Sprays on a Heated Plate," *International Journal of Heat and Mass Transfer*, Vol. 32, No. 10, 1989, pp. 1853–1864.

[16]Tilton, D. E., "Spray Cooling," Ph.D. Dissertation, Univ. of Kentucky, Lexington, KY, 1989.

[17]Pais, M. R., Chow, L. C., and Mahefkey, E. T., "Surface Roughness and Its Effects on the Heat Transfer Mechanism in Spray Cooling," *Journal of Heat Transfer*, Vol. 114, No. 1, 1992, pp. 211–219.

[18]Sehmbey, M. S., Pais, M. R., and Chow, L. C., "A Study of Diamond Laminated Surfaces in Evaporative Spray Cooling," *Thin Solid Films*, Vol. 212, Nos. 1–2, 1992, pp. 25–29.

[19]Toda, S., "A Study of Mist Cooling. 2nd Report: Theory of Mist Cooling and Its Fundamental Experiments," *Heat Transfer Japanese Research*, Vol. 3, No. 1, 1974, pp. 1–44.

[20]Bonacina, C., Comini, G., and Del Giudice, D., "Evaporation of Atomized Liquids on Hot Surfaces," *Letters in Heat and Mass Transfer*, Vol. 2, No. 5, 1975, pp. 401–406.

[21]Yang, J., Chow, L. C., Pais, M. R., and Ito, A., "Liquid Film Thickness and Topography Determination Using Fresnel Diffraction and Holography," *Journal of Experimental Heat Transfer*, Vol. 5, No. 3, 1992, pp. 239–252.

[22]Sehmbey, M. S., Pais, M. R., and Chow, L. C., "Effect of Surface Material Properties and Surface Characteristics in Evaporative Spray Cooling," *Journal of Thermophysics and Heat Transfer*, Vol. 6, No. 3, 1992, pp. 505–512.

[23]Yang, J., Pais, M. R., and Chow, L. C., "Critical Heat-Flux Limits in Secondary Gas Atomized Liquid Spray Cooling," *Journal of Experimental Heat Transfer*, Vol. 6, No. 1, 1993, pp. 55–67.

[24]Lefebvre, A. H., *Atomization and Sprays*, Hemisphere, New York, 1989, Chap. 6.

[25]Cooper, M. G., and Lloyd, J. P., "Transient Local Heat Flux in Nucleate Boiling," *Proceedings of the 3rd International Heat Transfer Conference* (Chicago, IL), Vol. 3, Science Press, Ephrato, PA, 1966, pp. 193–203.

[26]Mesler, R., "A Mechanism Supported by Extensive Experimental Evidence to Explain High Heat Fluxes Observed During Nucleate Boiling," *AIChE Journal*, Vol. 22, No. 2, 1976, pp. 246–252.

[27]Mesler, R., and Bellows, W. S., "Explosive Boiling: A Chain Reaction Involving Secondary Nucleation," *ASME Proceedings of the 1988 National Heat Transfer Conference*, Vol. 2, HTD-96, 1988, pp. 487–491.

[28]Mesler, R. B., "Improving Nucleate Boiling Using Secondary Nucleation," *Pool and External Flow Boiling*, edited by V. K. Dhir and A. E. Bergles, American Society of Mechanical Engineers Press, New York, 1992, pp. 43–47.

[29]Rohsenow, W. M., "Boiling," *Handbook of Heat Transfer Fundamentals*, edited by W. M. Rohsenow, J. P. Hartnett, and E. N. Ganić, 2nd ed., McGraw-Hill, New York, 1985, Chap. 12.